

1 **Supplemental Material for**  
2 **Rifamycin Resistance in *Clostridium difficile* is Generally Associated with a**  
3 **Low Fitness Burden**

4  
5 Uyen T. Dang<sup>1</sup>, Idalia Zamora<sup>1</sup>, Kirk E. Hevener<sup>2</sup>, Sudip Adhikari<sup>1</sup>, Xiaoqian Wu<sup>3</sup> and Julian G.  
6 Hurdle<sup>1,3,4\*</sup>

7 <sup>1</sup>Department of Biology, University of Texas at Arlington, Arlington Texas, 76019, USA;

8 <sup>2</sup>Biomedical and Pharmaceutical Sciences, College of Pharmacy, Idaho State University,

9 Meridian, Idaho, 83642, USA. <sup>3</sup>Center for Infectious and Inflammatory Diseases, Institute of

10 Biosciences and Technology, Texas A&M Health Science Center, Houston, Texas 77030, USA.

11 <sup>4</sup>Department of Microbial and Molecular Pathogenesis, Texas A&M Health Science Center,

12 College of Medicine, Bryan, Texas, 77807, USA.

13

14 \*Correspondence and requests for materials should be addressed to J.G.H

15 ([jhurdle@ibt.tamhsc.edu](mailto:jhurdle@ibt.tamhsc.edu)).

16

17

18

19

20

## 21 **COMPUTATIONAL METHODS**

22 ***CdRpoB* Homology Model.** A homology model of the *C. difficile* RNA polymerase subunit B  
23 (RpoB) was generated using the Schrödinger molecular modeling package (BioLuminate with  
24 Advanced Homology Modeling), the known *C. difficile* RpoB sequence (strain 630; accession  
25 no. CAJ66881.1), and the x-ray crystal structures of *E. coli* RNA polymerase in complex with  
26 rifampin (PDB ID 4KMU) (1, 2). ClustalW, interfaced from Schrödinger, was used to generate  
27 the sequence alignments between the RpoB subunit of the proteins (45% identity, 60% positives,  
28 15% gaps) (3). The knowledge-based model building method was used and rifampicin ligand  
29 from 4KMU was included in the model building. During model building, side chain rotamers  
30 were retained for conserved residues and optimized by minimization for residues not derived  
31 from the template. The structure of rifaximin was substituted for rifampin and minimized in  
32 place following the completion of the homology model.

33

34 ***CdRpoB* Mutations and Rifaximin Binding Energy Calculations.** The relative binding  
35 affinities (reported in kcal/mol) for rifaximin with the known resistance mutations in the  
36 *CdRpoB* model were calculated using the Prime MM-GBSA software included in the  
37 Schrödinger molecular modeling suite.(4) Prior to simulations the separated ligand (rifaximin)  
38 and protein were prepared using the Schrödinger protein preparation tool and as described above.  
39 The VSGB 2.0 solvation model and OPLS3 force field (both included in the Schrödinger  
40 software package, were used for the simulations. Protein flexible residues were permitted as  
41 defined by a 6 Å radius around the ligand (rifaximin) binding site. Full minimization sampling  
42 method was enabled. Relative binding affinities were calculated by comparing the MMGBSA

43 dG bind values for the native complex with those calculated for the resistance mutation  
44 complexes (**Table S1**, below).

45 *CdRpoB*/DNA structure preparation. The DNA & C-chain RpoB from *Thermus thermophilus*  
46 RNA polymerase x-ray crystal structure (4GZY) were aligned with the *CdRpoB* homology  
47 model using the Schrödinger/Maestro alignment software (5). Following this, the DNA subunit  
48 was transferred into the *CdRpoB* model and the complex was refined by restrained minimization  
49 using the OPLS3 force field with water solvation potential (extended cutoff, force field charges)  
50 with the Schrödinger software to a convergence of heavy atom RMSD 0.6 Å.

51

52

53

54

55

56

57

58

59

60

61

62

63

64

65

## 66 SUPPORTING RESULTS

### 67 Binding Energy Calculation Results

68 Modeling of binding energies for rifaximin to the homology model of *CdRpoB* is tabulated  
69 below. Modeling of *CdRpoB* containing double mutations as reported by Curry et al.(6) were  
70 performed. The R505K changes significantly impacts binding of rifaximin, but appears to lack  
71 an *in vitro* or *in vivo* fitness cost. It is unclear why second site mutations are required in mutants  
72 containing an R505K change or if R505K may act as a compensatory to other mutations.

73

74 **Table S1.** Changes in binding energy of rifaximin to *CdRpoB* for clinically relevant  
75 mutations/allelic sites.

Rifaximin- MM/GBSA Calculations		
Mutation	dG bind	ddG Native
WT	-105.578	0
S488Y	-68.762	36.816
D492Y	-85.357	20.221
H502N	-86.056	19.522
H502Y	-74.597	30.981
R505K	-52.112	53.466
S550F	-72.325	33.253
S550Y	-73.508	32.07
R505K/S488T	-54.677	50.901
R505K/I548K	-55.061	50.517
R505K/I548M	-67.615	37.963

76

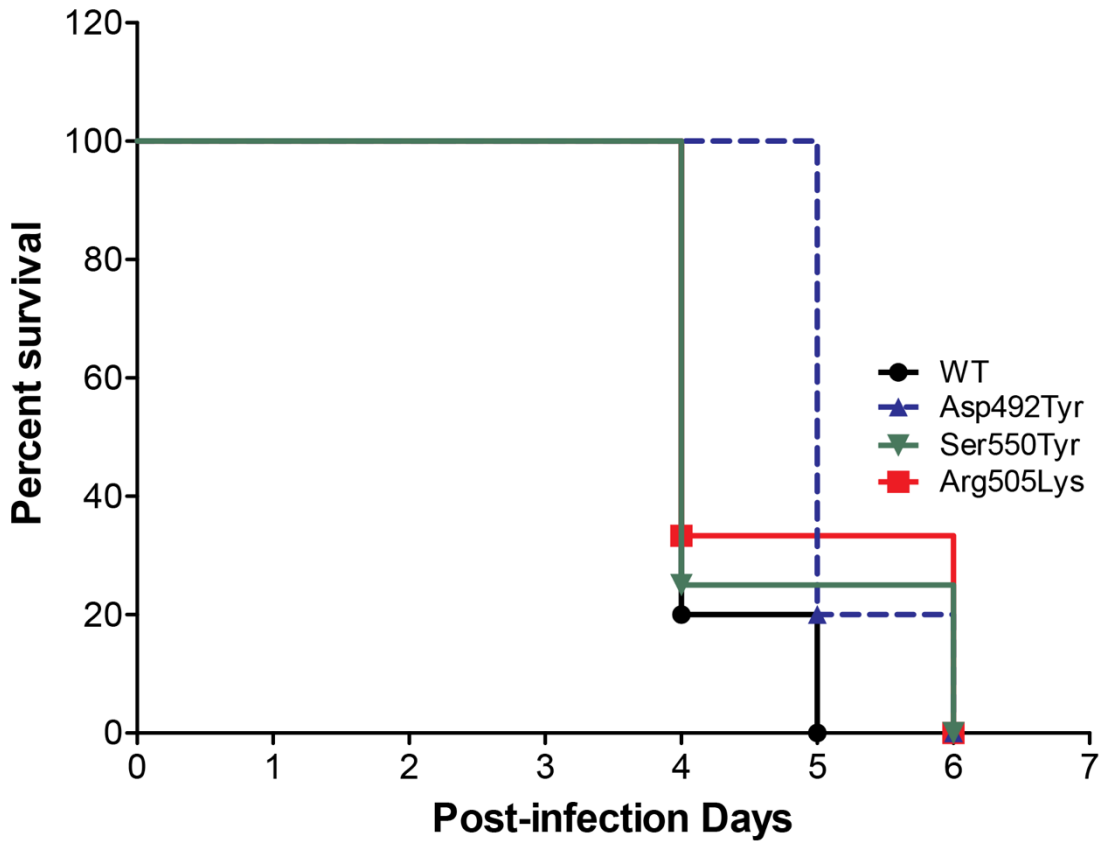
77 MM/GBSA = Molecular mechanics energies combined with generalized Born and surface area  
78 continuum solvation. dG= $\Delta G$ ; ddG=  $\Delta \Delta G$ = difference in Gibbs energy for ligand  
79 binding to WT and mutant.

80

81

82

83



84

85

86 **Figure S1.** Kaplan-Meier survival analysis of hamsters infected with wild type or rifaximin-

87 resistant mutants containing a point mutation. WT = parent strain CD43; Arg<sub>505</sub>Lys = mutant

88 strain CD43-D5; Asp<sub>492</sub>Tyr = mutant strain CD43-D3; and Ser<sub>550</sub>Tyr = mutant strain CD43-D9.

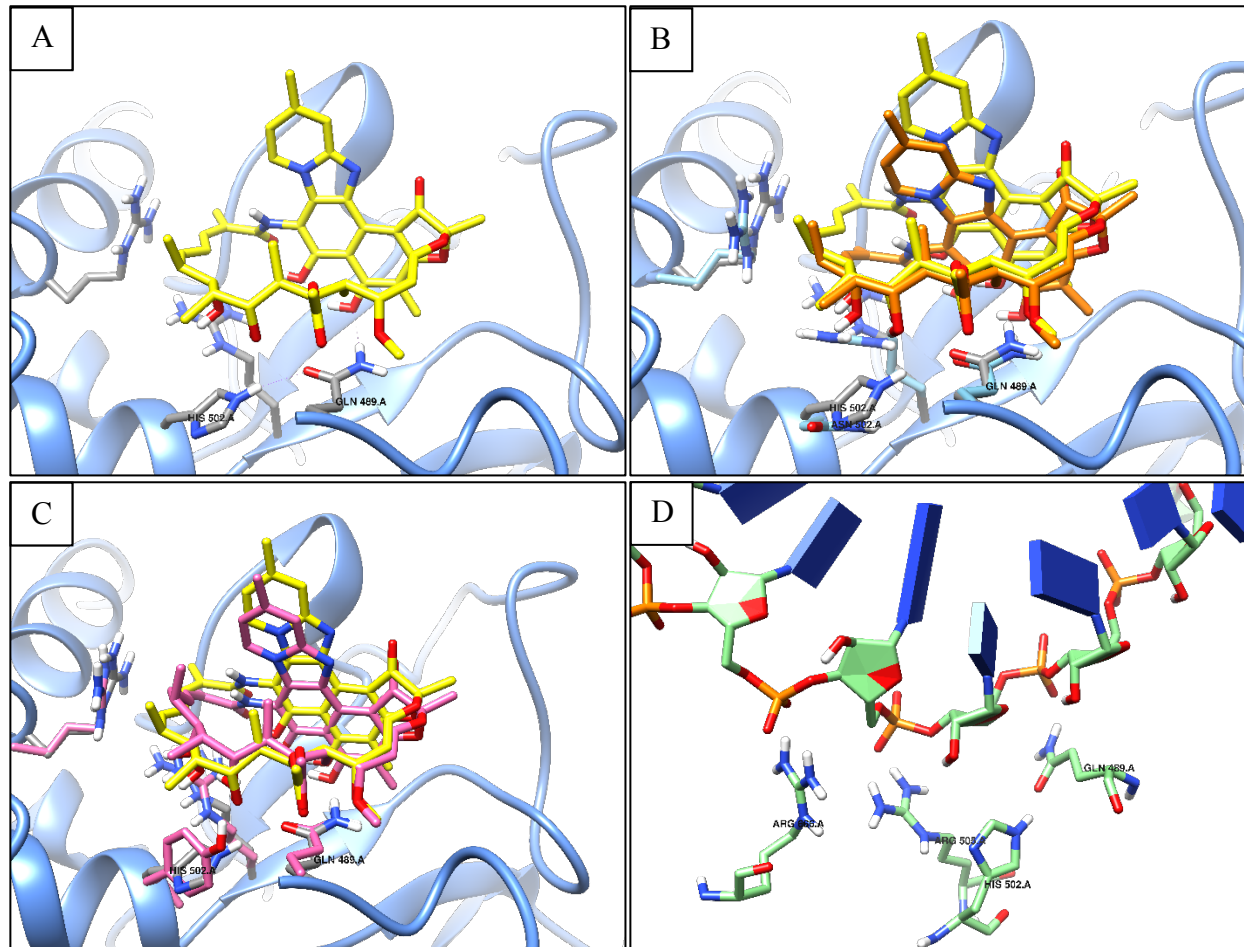
89 No significant differences exist between animal survival, as determined by Log-rank (Mantel-

90 Cox) Test (P=0.7366). The number of animals in each group were: n=5 for WT; n=6 for

91 Arg<sub>505</sub>Lys; n=5 for Asp<sub>492</sub>Tyr; and n=4 for Ser<sub>550</sub>Tyr.

92

94

95  
96

97 **Figure S2. H502 Mutation Interactions.** A. Native *CdRpoB* with bound rifaximin shows  
 98 hydrogen bonding network between H502, Q489, and phenolic –OH of rifaximin. B. H502N  
 99 mutation results in disruption of H-bond network in active site and movement of R505 leading to  
 100 minor positional changes in binding conformation of RFX (orange carbons). C. H502Y  
 101 mutation results in disruption of active site H-bond network and minor positional changes in  
 102 binding conformation of rifaximin (pink carbons). The Y502 hydroxyl group is predicted to  
 103 engage the rifaximin 10-position hydroxyl group in a hydrogen bond interaction. D. Model of  
 104 DNA bound to RpoB active site shows that H502 does not directly engage DNA backbone,  
 105 whereas R666, R505, and Q489 engage DNA backbone in electrostatic interactions.

106 **SUPPORTING REFERENCES**

- 107 1. **Molodtsov V, Nawarathne IN, Scharf NT, Kirchhoff PD, Showalter HD, Garcia GA,**  
108 **Murakami KS.** 2013. X-ray crystal structures of the *Escherichia coli* RNA polymerase  
109 in complex with benzoxazinorifamycins. *Journal of medicinal chemistry* **56**:4758-4763.
- 110 2. 2015. Biologics Suite 2015-3: Bioluminate, version 2.0. Schrödinger, LLC., New York,  
111 NY.
- 112 3. **Larkin MA, Blackshields G, Brown NP, Chenna R, McGettigan PA, McWilliam H,**  
113 **Valentin F, Wallace IM, Wilm A, Lopez R, Thompson JD, Gibson TJ, Higgins DG.**  
114 2007. Clustal W and Clustal X version 2.0. *Bioinformatics* **23**:2947-2948.
- 115 4. 2015. Schrödinger Release 2015-3: Prime, version 4.1. Schrödinger, LLC, New York,  
116 NY.
- 117 5. **Weixlbaumer A, Leon K, Landick R, Darst SA.** 2013. Structural basis of  
118 transcriptional pausing in bacteria. *Cell* **152**:431-441.
- 119 6. **Curry SR, Marsh JW, Shutt KA, Muto CA, O'Leary MM, Saul MI, Pasculle AW,**  
120 **Harrison LH.** 2009. High frequency of rifampin resistance identified in an epidemic  
121 *Clostridium difficile* clone from a large teaching hospital. *Clin. Infect. Dis.* **48**:425-429.

122